# Electrochemical Characterization and $CO_2$ Reduction Reaction of a family of Pyridazine-Bridged Dinuclear Mn(I) Carbonyl complexes.

Jacopo Isopi,[a] Elsa Quartapelle Procopio,[b] Lorenzo Veronese,[b] Marco Malferrari,[a] Giovanni Valenti,[a] Monica Panigati,[b,c] Francesco Paolucci,[a*] Massimo Marcaccio,[a*]

[a] *Dipartimento di Chimica "Giacomo Ciamician", Università di Bologna, via Selmi 2, 40126 Bologna, Italy;*

[b] *Dipartimento di Chimica, Università di Milano, via Golgi 19, 20133 Milano, Italy*

[c] *Consorzio INSTM, via G. Giusti 9, 50121, Firenze, Italy;*

*e-mail addresses*:

massimo.marcaccio@unibo.it

francesco.paolucci@unibo.it

## Abstract

Four neutral dinuclear carbonyl manganese complexes with pyridazine bridging ligand of general formula $[Mn_2(\mu\text{-}ER)_2(CO)_6(\mu\text{-}pydz)]$, (pydz = pyridazine, E = O or S; R = methyl or phenyl), recently synthesized, have been investigated by cyclic voltammetry in dimethylformamide and acetonitrile both under an inert argon atmosphere and in presence of carbon dioxide. This family of Mn(I) compounds show an interesting behaviour at negative potentials in presence of $CO_2$ which is herein discussed, by hypothesizing a rather efficient catalytic mechanism for the $CO_2$ reduction reaction toward the generation of CO.

## Introduction.

Owing to the fact that the applied potential to reduce $CO_2$ into its radical anion $CO_2^{\bullet-}$ has a rather negative value,[a,1] catalysts for the electrochemical $CO_2$ reduction reaction ($CO_2$RR) have been widely researched amongst the molecular metal-based systems, as transition metals generally have multiple redox states accessible that facilitate multielectron chemistry. The vast majority of these catalysts employ a single metal center,[2–8] usually rhenium or manganese. Albeit structurally similar, Re and Mn based catalysts show different electrochemical behavior. While rhenium complexes have been studied for longer time and historically thought to be the most efficient in $CO_2$RR, Chardon-Noblat, Deronzier and co-workers[9] evidenced that Mn complexes (where Mn center is typically in the Mn(I) oxidation state) can act as a good $CO_2$ reduction catalysts as well. Manganese based complexes have become the focus of intense investigation in recent years as pre-catalysts for $CO_2$ reduction, in part due to their high product selectivity for CO formation, but also because they are based on a cheaper and more earth-abundant metal, compared to their thoroughly investigated Re-based counterparts.

Mechanistic studies of rhenium-type catalysts have provided evidence for a concentration-dependent formation of dinuclear intermediates during catalysis.[10–15] However only few examples have been related to catalysts with a rigid bridging ligand that links two rhenium or two manganese active sites in close proximity with a predictable intermetallic distance and orientation,[16–18] in order to clearly highlight the contribution of the dinuclear pathway.[19,20] Indeed, cofacial dinuclear Re complexes with rigid backbone structure, that prevents Re-Re bonding (which leads to deactivation of carbon dioxide reduction catalysis), showed a beneficial interaction between the two reaction sites, clearly outperforming non-cofacial or mononuclear complexes at a double concentration. In this framework, it was recently reported by some of us, a new family of dinuclear tricarbonyl rhenium (I) complexes containing 1,2-diazine bridging ligand and halide anions, as ancillary ligands, and able to catalyze $CO_2$ reduction, with efficiency higher than that reported for the benchmark mononuclear complex $Re(CO)_3Cl$-(bpy), confirming that the use of dinuclear complexes could be very promising in this field.[21,22] Although efficiencies are lower than those reported by Jurss and co-worker for similar dinuclear Re complexes, (TOF = 15 $s^{-1}$ for our complex vs 35 $s^{-1}$ reported by Jurss)[19] our work highlights a crucial role of the catalyst structure, in terms of distance of the metal centers and capability to

[a] $E°(CO_2/CO_2^{\bullet-})$= –1.97 V versus SHE (standard hydrogen electrode) in DMF

allow the $CO_2$ insertion step.

These complexes belong to the recently reported family of dinuclear Re(I) complexes containing a 1,2-diazine bridging ligand and two anionic ancillary ligands, such as halides[23,24] hydrides[25] alcohoxides or chalcogenide[26,27] bridging between two $Re(CO)_3$ moieties.

On the basis of these results, we have recently synthetized a new similar family of dinuclear manganese complexes containing 1,2-diazine as bridging ligand and halides or chalcogenide as ancillary ligands (structural determination and a thorough characterization of all the compounds investigated in this work is reported elsewhere)[28] and having general formula $[Mn_2(\mu\text{-}ER)_2(CO)_6(\mu\text{-pydz})]$, (pydz = pyridazine, E = O or S; R = methyl or phenyl). Beside the rhenium counterpart, only two examples of dinuclear Mn complexes with two "$Mn(CO)_3$" moieties connected by only one aromatic nitrogen bridging ligand have been reported showing higher perfomances.[16,18] It is worth noting that dinuclear manganese complexes, as those here reported and containing not only the aromatic bridging ligand, but also two anionic bridging ligands, have been investigated for the efficient CO release[29–31] and as electrocatalysts for proton reduction,[32–34] but no examples have been reported for $CO_2$ reduction reaction.

In this work we have studied, for the first time, the electrochemical behaviour of this family of dinuclear Mn compounds (Scheme 1) in aprotic solvents and in presence of $CO_2$ to investigate its reduction reaction catalyzed by manganese based complexes and to explore the beneficial effects on the catalytic performances of such a dinuclear geometry inspired by similar works concerning rhenium.[21,22]

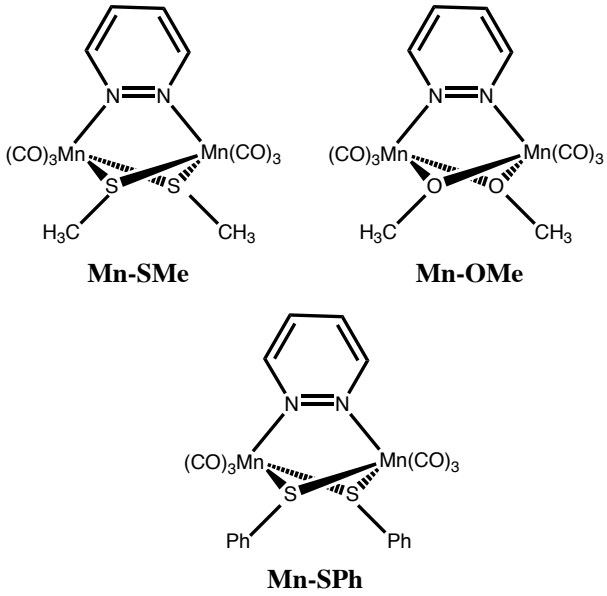


*Scheme 1.* Molecular structure of the investigated Mn(I) dinuclear complexes.

## Materials and Experimental Procedures.

Tetrabutylammonium hexafluoro-phosphate (TBAH) 99.0% from Sigma-Aldrich was used as electrolyte, N,N-dimethylformamide (DMF) 99.5% and acetonitrile (ACN) 99.5% as solvents both from Sigma-Aldrich. Electrochemical investigations by cyclic voltammetry (CV) were carried out using a BioLogic SP-300 instrument and a custom-made electrochemical cell. A 1 mm diameter GC disk was used as working electrode; the working electrode was polished with a 0.3 μm aluminium oxide (Buehler) slurry in distilled water on a felt pad. A Pt spiral wire acted as counter electrode and an Ag wire was used as pseudo-reference electrode that was checked to have a stable potential with a negligible drift within the time of experiment comprising several potential sweeps in the electrolyte/solvent used. The potential scale was corrected vs saturated calomel electrode (SCE) using the redox couple ferrocene/ferrocenium as internal reference. The solvent, both DMF and ACN, was purified and dried by distillation and stored over activated 4 Å molecular sieves in a Schlenk flask. It was transferred through a cannula system into a custom designed electrochemical cell containing the supporting electrolyte and the species under examination, immediately before performing the experiment.[22] The argon and carbon dioxide were initially bubbled through the electrolyte solution and during the measurements as a blanket of gas at a pressure of 1 bar.

All the $E_{½}$ potentials have been directly obtained from cyclic voltammetric curves as averages of the cathodic and anodic peak potentials and by digital simulation in the case of non-Nernstian or overlapping processes. Digital simulations of the cyclic voltammetric curves were carried out by Antigona[35] or DigiSim 3.0 (Bioanalytical Systems, Inc.), utilizing a best fitting procedure of the experimental curves recorded at different scan rates spanning over, at least, two orders of magnitude.[36,37]

The chalcogenide-bridged dinuclear Mn carbonyl complexes herein investigated (see Scheme 1) were obtained through the one-pot synthesis via "orthogonal bonding approach"[28] previously used for the synthesis of the analogue rhenium dinuclear complexes[27] and of different dinuclear manganese complexes.[30] The oxidative addition of $E_2R_2$ ligands (E = S and R = methyl or phenyl) to $Mn_2(CO)_{10}$ and the further addition of the pyridazine bridging ligand affords complexes labeled as **Mn-SMe**, **Mn-SPh** in good yields (about 60%). Concerning the synthesis of the methoxo-derivative **Mn-OMe**, methanol was used as source of $^-$OMe anions to get the corresponding managanese complex **Mn-OMe**. Structural determination of the products and the thorough characterization of all the compounds investigated in this work have been reported elsewhere.[28]

## Results and Discussion

Electrochemical investigation of compounds **Mn-OMe**, **Mn-SMe** and **Mn-SPh**, reported in Figure 1, was performed in DMF, which was preferred with respect to acetonitrile (ACN) in order to avoid the higher coordinating properties of ACN molecules to the metal center. Electrolyte solutions of about 1 mM of each of the three complexes studied were prepared using dry DMF and voltammetric measurement were carried out in inert atmosphere by Ar-saturating the solution. During the characterization procedures the sample solutions were kept in a dark environment for the whole time of the experiments as Mn complexes are liable to photodegradation. All the systems were electrochemically characterized in a wide potential window by using a glassy carbon disk under the inert Ar-atmosphere (Figure 1), before the introduction of the $CO_2$; the potentials of the most significant processes are reported in Table 1.

Herein, the voltammetric behaviour of an Ar-saturated solution of the species **Mn-OMe**, **Mn-SMe** and **Mn-SPh** has been prevalently investigated in the negative potential range, as

shown in Figure 1. For **Mn-SMe** and **Mn-OMe**, (Figure 1a and 1b respectively) the potential scan at negative values presents a completely reversible reduction with a half wave potential $E_{1/2}^{I}$ at about -1.0 V (*vs* SCE) and centered on the diazine ligand (*vide infra*). The reversibility of this peak clearly indicates a good stability of these complexes towards processes involving ligand dissociation and the further formation of dimers containing Mn-Mn bond, usually observed in the reduction of mononuclear tricarbonyl Mn complexes.[9,38,39]

The first reduction is followed by a second voltammetric wave with a two-electron peak at about -2.3 V, which occurs just at the edge of the potential window allowed by the solvent. This last voltammetric peak, is completely irreversible and only a careful inspection of the voltammetric features highlights the presence of two subsequent overlapping processes with potentials very closely spaced (labeled as II and III in Figure 1a). Moreover, on the backward potential scan it spawns three small reoxidation processes with peak potentials reported in Table 1, thus suggesting a reaction mechanism of the molecule, following up the second reduction voltammetric peak (*vide infra*, description of the mechanism). In the case of **Mn-OMe** two other smaller reduction peaks are observed at -0.9 V and -2.2 V respectively (indicated with asterisks in Figure 1b) that are related to the reduction of some decomposition products. Actually, although all the CV experiments were carefully carried out in dark conditions, **Mn-OMe** derivative resulted to be highly photosensitive, even upon exposition to indirect sunlight, making impossible the prevention of some partial decomposition. The photostability of the complexes in different solvents has been investigated and fully reported elsewhere.[28]

Figure 1c reports the electrochemical behaviour of species **Mn-SPh,** for which the reversibility of the first peak is plenty lost. This is in agreement with the weaker donating power of the phenylsulfide anion with respect to the methylsulfide or to the methoxo anions. This leads to a weakening of the Mn-S bond, resulting in a possible opening of the bridge bond, formed by the ancillary ligands, and thus a partial dissociation of the complex. As a consequence, the two-electron voltammetric wave beyond -2.0 V is split into two distinct one-electron processes.

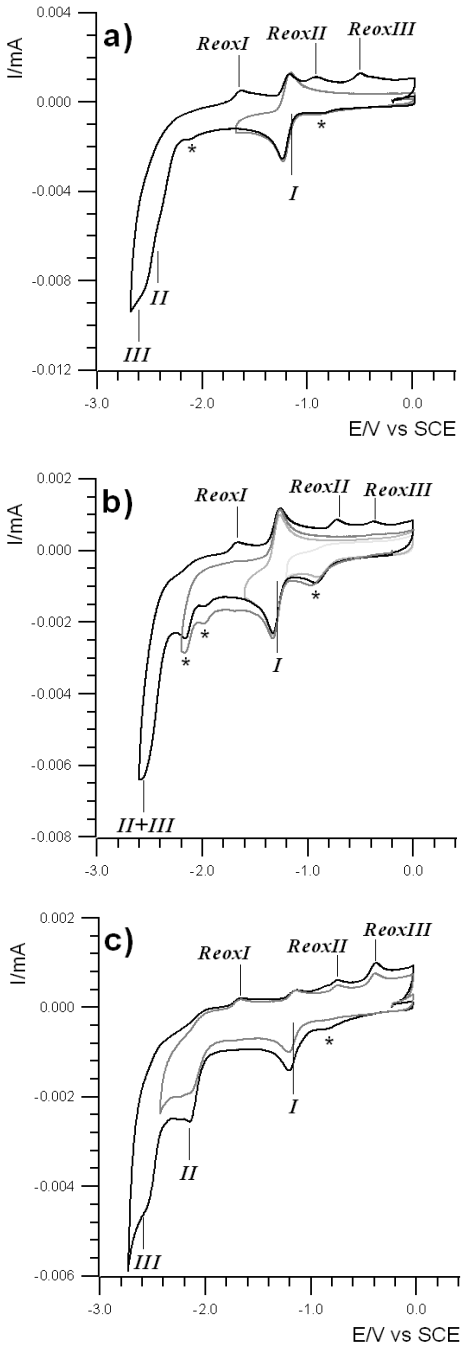


*Figure 1.* Cyclic voltammetry curves in Ar atmosphere of **Mn-SMe** (a), **Mn-OMe** (b), **Mn-SPh** (c) Solvent: DMF, scan rate: 0,4 V/s; T = 298K.

*Table 1.* Half-Wave ($E_{1/2}$) and peak redox potentials (vs SCE) of compounds recorded in TBAH/DMF solution at 25 °C.

| ***Species*** | $E_{1/2}$ or $E_p$/ V (reduction) | | | $E_p$/ V (re-oxidation) | | |
|---|---|---|---|---|---|---|
| | ***I*** | ***II*** | ***III*** | ***ReoxI*** | ***ReoxII*** | ***ReoxIII*** |
| **Mn-SMe** | -1.20 | -2.44[a]; | -2.56[a] | -1.62[a] | -0.92[a] | -0.50[a] |
| **Mn-OMe** | -1.30 | -2.52[a] | -2.60[a] | -1.68[a] | -0.72[a] | -0.36[a] |
| **Mn-SPh** | -1.18 | -2.14[a] | 2.58[a] | -1.68[a] | -0.74[a] | -0.38[a] |

[a] Peak potential

To shed light on the behavior seen in Ar saturated DMF electrolyte solution, simulations were performed to understand a possible undergoing mechanism. In order to obtain a set of reliable and acceptable thermodynamic and kinetic parameters for the hypothesized mechanism (*vide infra*) the fit of the experimental voltammetric curves were obtained within a two-order-of-magnitude range of scan rates (between 0.4 and 10 V/s). Data for the **Mn-SMe** sample are reported below, in Figure 2.

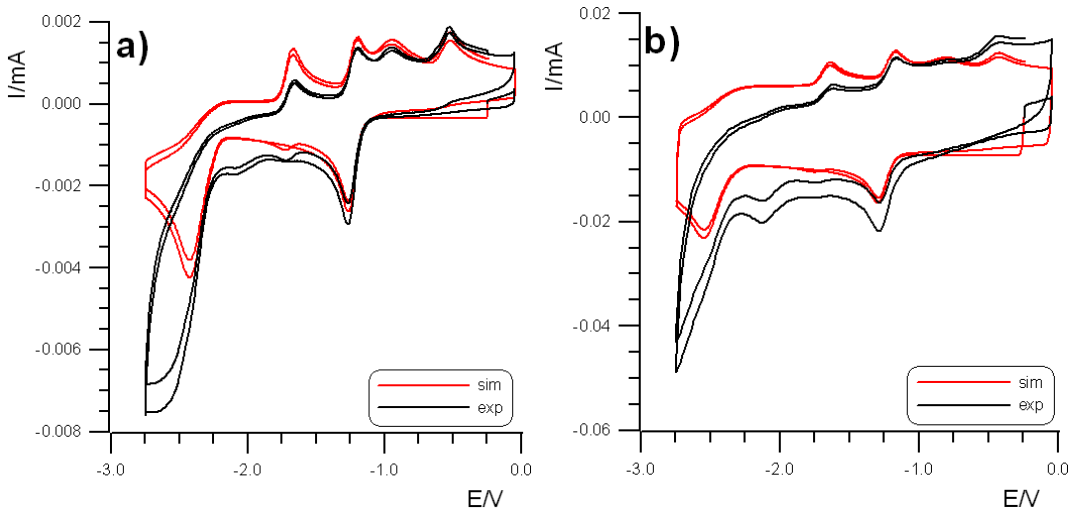


*Figure 2.* Simulated voltammetric curves (Antigona software) juxtaposed on the original experimental data of Mn-**SMe**. Simulations parameters fitted using experimental CVs with scan rate 0.4 V/s (a) and 10.0 V/s (b). Ar atmosphere, TBAH/DMF electrolyte solution, working electrode: GC; reference electrode: SCE; T= 298 K

On the basis of the electrochemical and chemical behaviour of the various species, the electrochemical mechanism, that reasonably fits the experimental data, is sketched below in Scheme 2 and the electrochemical and chemical simulation parameters are reported in Table S-1 in the Supporting Information. In particular it shows a reversible one-electron process followed by an irreversible two closely spaced one-electron reductions. This second process leads to three different oxidation peaks on the reverse anodic scan back to the initial potential.

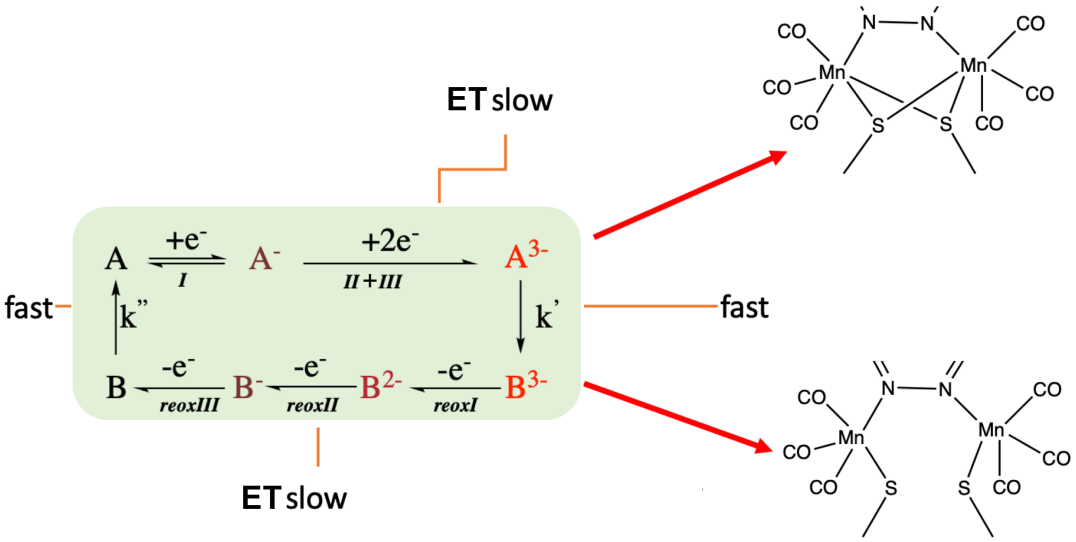


*Scheme 2.* Simplified mechanism proposed to rationalize the experimental CV data obtained and to simulate the voltammetric curves of **Mn-SMe** in DMF solution. Double and single orizontal half arrows represent electron transfers and full vertical arrows represent chemical reactions. The E° values for the various electron transfers and the kinetic constants of reactions are estimated from the simulation.

The first reversible process can be reasonably attributed to the reduction of the aromatic diazine ring, not inducing any bond breaking. The irreversibility of the second voltammetric process (comprising two close one-electron transfers) indicates that the doubly and triply reduced molecule is becoming unstable and a following up chemical reaction occurs. It can be associated to the double reduction of the two metal centers and this has, most likely, a chemical consequence consisting in the partial breaking of the sulfur-Mn bonds between the ancillary bridging ligands and the Mn nuclei.

In this respect, some preliminary molecular orbital DFT calculations on the **Mn-SMe**

species have been carried out confirming that the first reduction is mostly centred on the diazine bridging ligand, while the subsequent two electron injections are mainly metal-centred. Moreover, while the molecular structure optimization at M06/3-21G* level of the theory, for the first reduced species **Mn-SMe**, does not show any significant Mn-S bond elongation (only 0.02 Å), when the second electron is added, the optimization of the 2-electron reduced molecular structure evidences a rather large increase (0.22 Å) in one of the two Mn-SR bridging bonds for both the ancillary ligands. Such a 0.22 Å value is undoubtedly a clear indication and a theoretical support to the "opening" of the ancillary bridges (see Figure S-1 in the Supporting Information).

From the new formed *isomeric* structure (right-bottom structure in Scheme 2), the re-oxidation to the original valence state is possible and the processes are again irreversible because the electron transfers are affected by chemical reactions. In fact, this last chemical process leads to re-establish the bonds involving the bridging sulfurs, thus originating a square-scheme mechanism as sketched in Scheme 2. Thus, such a reaction mechanism can be involved in the interaction with $CO_2$ and its reduction (*vide infra*). It should be noted that voltammetric curves recorded at lower scan rates (<0.4 V/s) show some degree of an electrode passivation.

***Electrocatalysis.*** After the preliminary voltammetric investigation in inert atmosphere, the solution was saturated with $CO_2$. The presence of $CO_2$ leads to a remarkable change in the voltammetric pattern with an increase in the current of the two electron peak occurring at potential more negative than -2.0 V, for all the four systems, thus indicating that the highly reduced transient species, electrogenerated at those potentials, are affected in some way by the presence of carbon dioxide. Such an increase of the current wave overlaps with the two-electron peak (i.e., processes ***II***+***III***) and overwhelms it with an apparent anticipation of what looks like a solvent discharge, as shown in Figure 3 for all the Mn complexes. Moreover, it is worth to observe the complete absence of the sequence of the three reoxidation processes on the reverse anodic scan, thus suggesting that the new process completely overturns the previously detected one in argon (Figure 3).

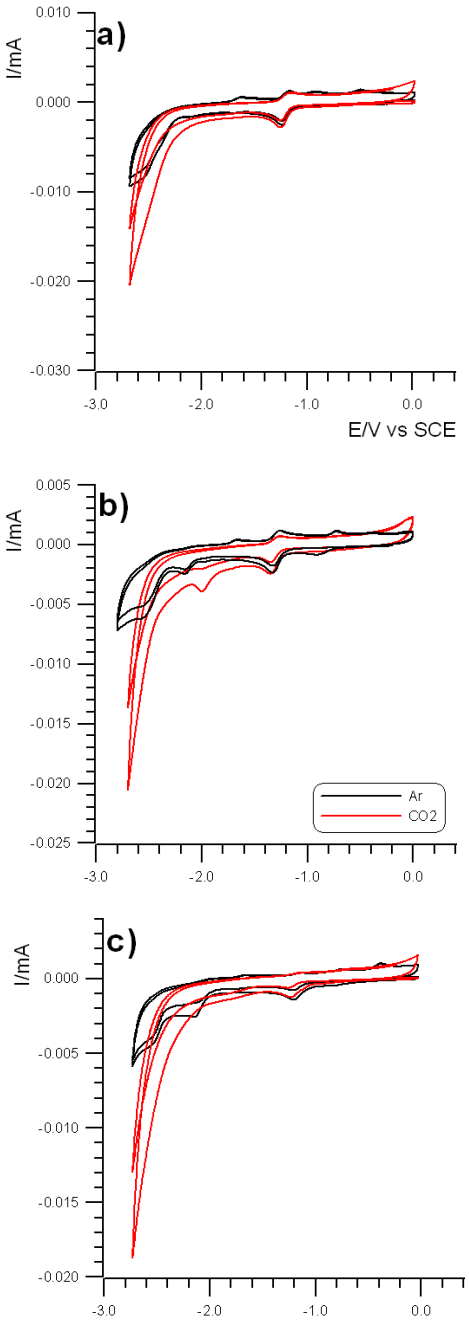


*Figure 3.* Cyclic voltammetry comparison between sample behavior in Ar (black) and in $CO_2$ (red) saturated solution of **Mn-OMe** (a), **Mn-SMe** (b), **Mn-SPh** (c) in DMF. Working electrode: GC ($7.85\times10^{-3}$ $cm^2$); reference electrode: SCE; scan rate: 0.4 V/s; T= 298K.

A very similar voltammetric behavior was observed also in acetonitrile solution. Figure 4 reports the CV curves of all the complexes in ACN in the presence of $CO_2$ revealing a strong current increase at the second reduction peak potential, as observed in DMF solution.

For the sake of comparison, a blank experiment without any of the manganese complexes in solution revealed that $CO_2$ reduction was observed on a glassy carbon electrode only starting at – 2.6 V, with a shift of ~0.4–0.5 V towards more negative potential.

Measurements showing a clear and efficient $CO_2$RR, in particular for the dinuclear carbonyl Mn species **Mn-SMe**, and **Mn-SPh**, allowed the calculation of the Turnover Frequency (TOF) for such systems. By comparing the relevant peak current in presence of the substrate $CO_2$ ($i_{cat}$) and in its absence ($i_p$) it is possible to calculate the TOF for a homogeneous catalyst (in the case of a reversible electron-transfer reaction followed by a fast catalytic reaction) using equations:

$$i_{cat} = n_{cat} F A [cat] (D k_{cat} [Q]^{y})^{1/2} \quad (1)$$

$$i_p = 0.4463 n_p^{3/2} F A [cat] \left(\frac{F}{RT}\right)^{1/2} v^{1/2} D^{1/2} \quad (2)$$

$$TOF = k_{cat}[Q] \quad (3)$$

where $y$ is equal to 1, assuming a pseudo-first-order kinetics, since the concentrations of the substrate Q (i.e., $CO_2$) is large in comparison to the concentration of catalyst.[40] Moreover, $n_{cat}$ is the number of electrons required for the catalytic reaction ($n_{cat}$ = 2 for the reduction of $CO_2$ to CO), F is the Faraday's constant, A is the surface area of the electrode, [cat] is the catalyst concentration, D is the diffusion constant of the catalytically-active species, $k_{cat}$ is the rate constant of the catalytic reaction, and [Q] is the substrate concentration. Equation 2 describes the peak current of a reversible electron transfer not affected by any following-up reaction.[41] R is the universal gas constant, T is temperature, $n_p$ is the number of electrons in the reversible non-catalytic reaction, and υ is scan rate. Dividing eq 1 by eq 2 allows for the determination of $i_{cat}/i_p$ and the further calculation of the catalytic rate constant ($k_{cat}$) and the turnover frequency (TOF). Solving $i_{cat}/i_p$ for $k_{cat}[Q]$ and combining with equation 3 it is possible to get:

$$TOF = k_{cat}[Q] = \frac{F v n_p^3}{RT} \left(\frac{0.4463}{n_{cat}}\right)^2 \left(\frac{i_{cat}}{i_p}\right)^2 \quad (4)$$

In this equation, the factor A cancels out because the same electrode was used for the experiments under $CO_2$ and Ar. The diffusion coefficient D also cancels out because we

are assuming that the value of the catalytically-active species does not change significantly under $CO_2$ or Ar. By using experimental data from ACN solutions of Mn-**SMe** and Mn-**SPh** (Figure 4) the TOF values were calculated through eq 4.

Using the current peaks of the first voltammetric cycle (to exclude any eventual electrode passivation) TOF values are 131 $s^{-1}$ for **Mn-SMe** and 10 $s^{-1}$ for **Mn-SPh**. Data from **Mn-SMe** and **Mn-SPh** show them behaving much above the value reported in previous works on manganese-based systems of 7.2 $s^{-1}$.[42] Scans done on **Mn-OMe** provide evidence that this Mn complex is inactive toward the CO2RR.

The notable large difference of activity between the O-based and S-based bridging moieties for the two systems **Mn-OMe** and **Mn-SMe**, respectively, represents a proof of the influence of the ancillary ligand on the catalytic performances, as reported for the analogous rhenium complexes.[22] In **Mn-SMe** both Mn-S bonds cleavage take place almost simultaneously, without decomposition of the complex and/or formation of Mn-Mn direct bond, making both the metal centers available to interact with $CO_2$, as sketched in Scheme 3. It is unlikely that two $CO_2$ molecules have enough room to interact independently with both nuclei, but, as previously reported in literature, a dinuclear reaction site can outperform two independent mononuclear ones, as demonstrated on Re-based systems.[19]

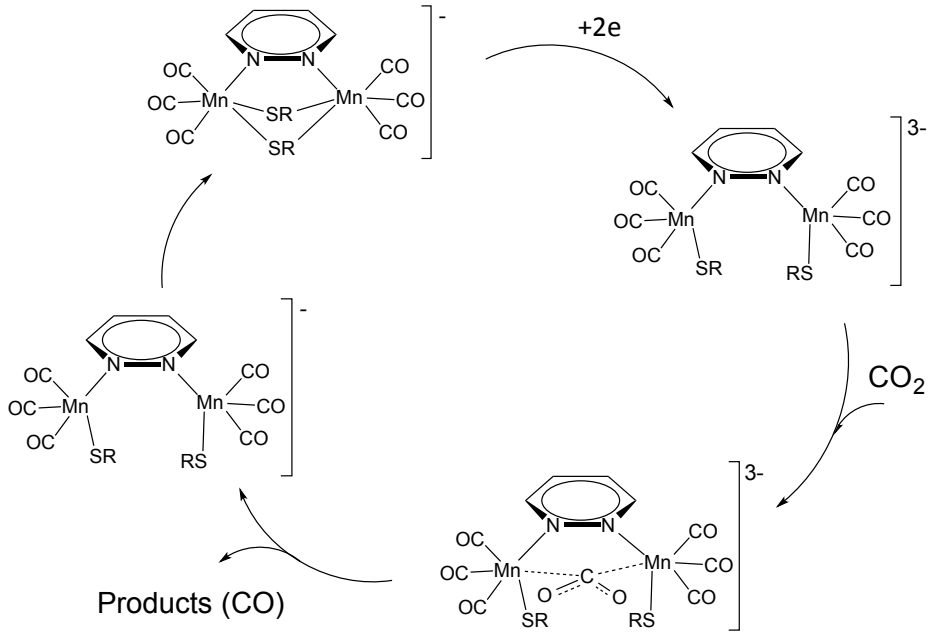


Scheme 3. *Sketch of the mechanism proposed for the catalysis of the $CO_2$ reduction reaction by the **Mn-SMe** complex.*

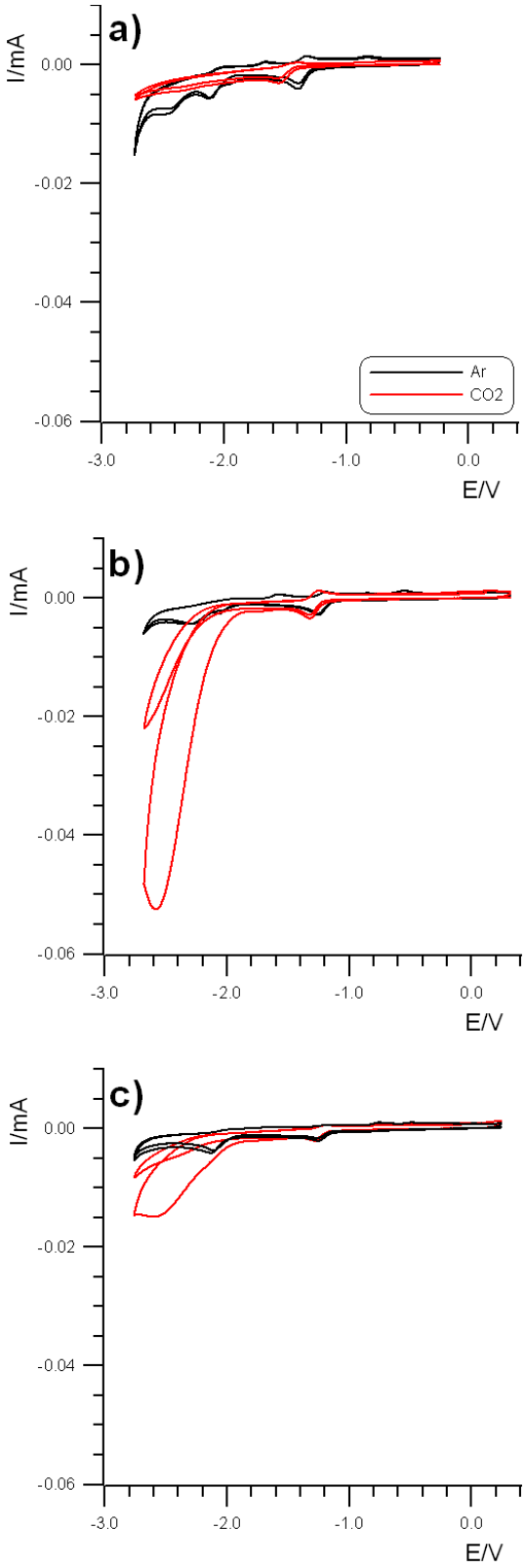


*Figure 4.* Comparison of the voltammetric behavior between **Mn-OMe** 0.6 mM (a), **Mn-SMe** 0.9 mM (b), **Mn-SPh** 0.3 mM (c) in TBAH/ACN electrolyte solution in presence of Ar (black traces) and $CO_2$ (red traces). Working Electrode: GC disk ($7.85\times10^{-3}$ $cm^2$); Reference Electrode: SCE; scan rate ($\upsilon$): 0.4 V/s; T= 298K.

However, in **Mn-SPh**, the two Mn-S bond cleavage can give rise to a partial decomposition of the complex, due to the lower donating power of the phenyl derivative, and splitting the second voltammetric peak in two processes. Interestingly, the $CO_2$RR peak takes place clearly when the species with one metal center, formed upon reduction, is available for interaction with the substrate. On the other hand, the strong interaction of $OMe^-$ anion with the metal center, due to the hard nature of the ligand and its higher electronegativity, with respect to the $SMe^-$ anion, could partially hamper the coordination of $CO_2$ thus decreasing the efficiency.

## Conclusions

We have described and electrochemically characterized three manganese complexes, having different bridging ancillary chalcogenide ligands, as promising homogeneous $CO_2$RR catalysts. As the analogous rhenium complexes, the catalysis efficiency, quantified by using literature methods, confirms the strong correlation between molecular structure and catalytic activity in $CO_2$ reduction. The maximum TOF was observed for complex **Mn-SMe**, affording an impressive $CO_2$RR activity with TOF values up of 131 $s^{-1}$ that is much above those reported by previous works on manganese-based systems, reaching a maximum of 7.2 $s^{-1}$. The three order of magnitude of difference between the two very similar systems can give a further interesting insight into the mechanism taking place at the reaction site, showing the effect of the ancillary ligand on catalytic activity. A mechanism has been hypothesized on the basis of the electrochemical findings indicating that the reaction site for $CO_2$RR is formed when the bond with the ancillary bridging ligand is cleaved so that the $CO_2$ molecule can access the metal center. In particular, this feature is in agreement with the lower electronegativity of the sulfur, with respect to the oxygen, together with the higher donor power of methyl with respect to phenyl, that increases the electronic density on the Mn centers and the stability of the reduced species, thus increasing the catalytic activity.

## Aknowledgments

This research was supported by the Università di Bologna, Università di Milano, the Italian Ministero dell'Università e Ricerca – MIUR and INSTM.

## References


1. Amatore, C. & Saveant, J. M. Mechanism and Kinetic Characteristics of the Electrochemical Reduction of Carbon Dioxide in Media of Low Proton Availability. *J. Am. Chem. Soc.* **103**, 5021–5023 (1981).

2. Benson, E. E., Kubiak, C. P., Sathrum, A. J. & Smieja, J. M. Electrocatalytic and homogeneous approaches to conversion of $CO_2$ to liquid fuels. *Chem. Soc. Rev.* **38**, 89–99 (2009).

3. Yui, T., Tamaki, Y., Sekizawa, K. & Ishitani, O. Photocatalytic Reduction of $CO_2$: From Molecules to Semiconductors. in 151–184 (2011). doi:10.1007/128_2011_139.

4. Finn, C., Schnittger, S., Yellowlees, L. J. & Love, J. B. Molecular approaches to the electrochemical reduction of carbon dioxide. *Chem. Commun.* **48**, 1392–1399 (2012).

5. Appel, A. M. *et al.* Frontiers, Opportunities, and Challenges in Biochemical and Chemical Catalysis of $CO_2$ Fixation. *Chem. Rev.* **113**, 6621–6658 (2013).

6. Kang, P., Chen, Z., Brookhart, M. & Meyer, T. J. Electrocatalytic Reduction of Carbon Dioxide: Let the Molecules Do the Work. *Top. Catal.* **58**, 30–45 (2015).

7. Takeda, H., Cometto, C., Ishitani, O. & Robert, M. Electrons, Photons, Protons and Earth-Abundant Metal Complexes for Molecular Catalysis of $CO_2$ Reduction. *ACS Catal.* **7**, 70–88 (2017).

8. Francke, R., Schille, B. & Roemelt, M. Homogeneously Catalyzed Electroreduction of Carbon Dioxide—Methods, Mechanisms, and Catalysts. *Chem. Rev.* **118**, 4631–4701 (2018).

9. Bourrez, M., Molton, F., Chardon-Noblat, S. & Deronzier, A. [Mn(bipyridyl)(CO)3Br]: An Abundant Metal Carbonyl Complex as Efficient Electrocatalyst for $CO_2$ Reduction. *Angew. Chemie Int. Ed.* **50**, 9903–9906 (2011).

10. Breikss, A. I. & Abruña, H. D. Electrochemical and mechanistic studies of $Re(CO)_3$(dmbpy)CI] and their relation to the catalytic reduction of $CO_2$. *J. Electroanal. Chem. Interfacial Electrochem.* **201**, 347–358 (1986).

11. Sullivan, B. P., Bolinger, C. M., Conrad, D., Vining, W. J. & Meyer, T. J. One- and

two-electron pathways in the electrocatalytic reduction of $CO_2$ by fac-Re(bpy)$(CO)_3$Cl (bpy = 2,2′-bipyridine). *J. Chem. Soc., Chem. Commun.* 1414–1416 (1985) doi:10.1039/C39850001414.

12. Deronzier, A. *et al.* Photoredox pathways for the polymerization of a pyrrole-substituted ruthenium tris(bipyridyl) complex. *New J. Chem.* **22**, 33–37 (1998).

13. Smieja, J. M. *et al.* Manganese as a Substitute for Rhenium in $CO_2$ Reduction Catalysts: The Importance of Acids. *Inorg. Chem.* **52**, 2484–2491 (2013).

14. Wilting, A. & Siewert, I. A Dinculear Rhenium Complex with a Proton Responsive Ligand in the Electrochemical-Driven $CO_2$ -Reduction Catalysis. *ChemistrySelect* **3**, 4593–4597 (2018).

15. Liyanage, N. P. *et al.* Photochemical $CO_2$ reduction with mononuclear and dinuclear rhenium catalysts bearing a pendant anthracene chromophore. *Chem. Commun.* **55**, 993–996 (2019).

16. Siewert, I. Electrochemical $CO_2$ Reduction Catalyzed by Binuclear L$Re_2(CO)_6Cl_2$ and L$Mn_2(CO)_6Br_2$ Complexes with an Internal Proton Source. *Acc. Chem. Res.* **55**, 473–483 (2022).

17. Mukherjee, J. & Siewert, I. Manganese and Rhenium Tricarbonyl Complexes Equipped with Proton Relays in the Electrochemical $CO_2$ Reduction Reaction. *Eur. J. Inorg. Chem.* **2020**, 4319–4333 (2020).

18. Cohen, K. Y. *et al.* Elucidating the mechanism of photochemical $CO_2$ reduction to CO using a cyanide-bridged di-manganese complex. *Dalt. Trans.* **51**, 17203–17215 (2022).

19. Yang, W. *et al.* Electrocatalytic CO2 Reduction with Cis and Trans Conformers of a Rigid Dinuclear Rhenium Complex: Comparing the Monometallic and Cooperative Bimetallic Pathways. *Inorg. Chem.* **57**, 9564–9575 (2018).

20. Giereth, R. *et al.* Elucidation of Cooperativity in $CO_2$ Reduction Using a Xanthene-Bridged Bimetallic Rhenium(I) Complex. *ACS Catal.* **11**, 390–403 (2021).

21. Valenti, G. *et al.* Diazine bridged dinuclear rhenium complex: New molecular material for the $CO_2$ conversion. *Inorganica Chim. Acta* **417**, 270–273 (2014).

22. Quartapelle Procopio, E. *et al.* Dinuclear Re(I) Complexes as New Electrocatalytic Systems for $CO_2$ Reduction. *ChemElectroChem* **8**, 2065–2069 (2021).

23. Donghi, D. *et al.* A New Class of Luminescent Tricarbonyl Rhenium(I) Complexes Containing Bridging 1,2-Diazine Ligands: Electrochemical, Photophysical, and Computational Characterization. *Inorg. Chem.* **47**, 4243–4255 (2008).

24. Panigati, M. *et al.* Luminescent dinuclear rhenium(I) complexes containing bridging 1,2-diazine ligands: Photophysical properties and application. *Coord. Chem. Rev.* **256**, 1621–1643 (2012).

25. Panigati, M. *et al.* Luminescent Hydrido-Carbonyl Clusters of Rhenium Containing Bridging 1,2-Diazine Ligands. *Inorg. Chem.* **45**, 10909–10921 (2006).

26. Raimondi, A. *et al.* Electrochemical, Computational, and Photophysical Characterization of New Luminescent Dirhenium–Pyridazine Complexes Containing Bridging OR or SR Anions. *Inorg. Chem.* **51**, 2966–2975 (2012).

27. Veronese, L., Quartapelle Procopio, E., Maggioni, D., Mercandelli, P. & Panigati, M. Dinuclear rhenium pyridazine complexes containing bridging chalcogenide anions: synthesis, characterization and computational study. *New J. Chem.* **41**, 11268–11279 (2017).

28. Panigati, M. *et al. New dinuclear tricarbonyl Mn(I) complexes containing 1,2 bridging diazine ligands: synthesis, characterization and redox chemistry.* manuscript under submission (Jan. 2023).

29. Divya, D., Nagarajaprakash, R., Vidhyapriya, P., Sakthivel, N. & Manimaran, B. Single-Pot Self-Assembly of Heteroleptic Mn(I)-Based Aminoquinonato-Bridged Ester/Amide-Functionalized Dinuclear Metallastirrups: Potential Anticancer and Visible-Light-Triggered CORMs. *ACS Omega* **4**, 12790–12802 (2019).

30. Kumar, U. *et al.* Selenolato-Bridged Manganese(I)-Based Dinuclear Metallacycles as Potential Anticancer Agents and Photo-CORMs. *ACS Omega* **4**, 1923–1930 (2019).

31. Kumar, U. *et al.* Self-assembly of manganese(I) based thiolato bridged dinuclear metallacycles: synthesis, characterization, cytotoxicity evaluation and CO-releasing studies. *New J. Chem.* **43**, 7520–7531 (2019).

32. Hou, K., Lauw, S. J. L., Webster, R. D. & Fan, W. Y. Electrochemical proton reduction catalysed by selenolato-manganese carbonyl complexes. *RSC Adv.* **5**, 39303–39309 (2015).

33. Hou, K. & Fan, W. Y. Electrocatalytic proton reduction catalyzed by a dimanganese disulfide carbonyl complex containing a redox-active internal disulfide bond. *Dalt. Trans.* **43**, 16977–16980 (2014).

34. Kaim, V., Natarajan, M. & Kaur□Ghumaan, S. Dinuclear Manganese Carbonyl Complexes: Electrocatalytic Reduction of Protons to Dihydrogen. *ChemistrySelect* **4**, 1789–1794 (2019).

35. Mottier, L. *Antigona*, University of Bologna, Bologna, Italy, 1999.

36. Alberti, A. *et al.* An ESR and electrochemical approach to the unusual reactivity of ferrocenoylsilanes with organometallic compounds. *J. Phys. Org. Chem.* **17**, 1084–1090 (2004).

37. Mateo-Alonso, A. *et al.* An electrochemically driven molecular shuttle controlled and monitored by $C_{60}$. *Chem. Commun.* 1945-1947 (2007).

38. Scherpf, T. *et al.* A Mesoionic Carbene–Pyridine Bidentate Ligand That Improves Stability in Electrocatalytic $CO_2$ Reduction by a Molecular Manganese Catalyst. *Inorg. Chem.* **61**, 13644–13656 (2022).

39. Grills, D. C., Ertem, M. Z., McKinnon, M., Ngo, K. T. & Rochford, J. Mechanistic aspects of $CO_2$ reduction catalysis with manganese-based molecular catalysts. *Coord. Chem. Rev.* **374**, 173–217 (2018).

40. Sampson, M. D. *et al.* Manganese Catalysts with Bulky Bipyridine Ligands for the Electrocatalytic Reduction of Carbon Dioxide: Eliminating Dimerization and Altering Catalysis. *J. Am. Chem. Soc.* **136**, 5460–5471 (2014).

41. Bard J. Allen, F. R. L. *ELECTROCHEMICAL METHODS: Fundamental and Applications*. (Wiley-VCH Verlag GmbH & Co. KGaA, 2000).

42. Riplinger, C., Sampson, M. D., Ritzmann, A. M., Kubiak, C. P. & Carter, E. A. Mechanistic contrasts between manganese and rhenium bipyridine electrocatalysts for the reduction of carbon dioxide. *J. Am. Chem. Soc.* **136**, 16285–16298 (2014).